

1 ***Quantifying the impact of lagged hydrological responses on the effectiveness of groundwater***
2 ***conservation***

3
4 **Authors:** Thomas J Glose¹, Samuel C Zipper¹, David W Hyndman^{2,3}, Anthony D Kendall³,
5 Jillian M Deines⁴, James J Butler, Jr.¹

6
7 **Affiliations:**

8 1. Kansas Geological Survey, University of Kansas, Lawrence KS, 66047, USA

9 2. School of Natural Sciences and Mathematics, University of Texas at Dallas, Richardson, TX,
10 75080, USA

11 3. Department of Earth and Environmental Sciences, Michigan State University, East Lansing,
12 MI, 48824, USA

13 4. Department of Earth System Science and Center on Food Security and the Environment,
14 Stanford University, Stanford, CA, 94035, USA

15
16 **Corresponding Author:** tomglose@ku.edu

17
18 **Author ORCID IDs:**

19 Glose: 0000-0002-5414-3571

20 Zipper: 0000-0002-8735-5757

21 Hyndman: 0000-0001-9464-8403

22 Kendall: 0000-0003-3914-9964

23 Deines: 0000-0002-4279-8765

24 Butler: 0000-0002-6682-266X

25
26 This is a manuscript in revision following peer review at *Water Resources Research*.

27
28 **Keywords:** numerical modeling, lagged processes, groundwater conservation, pumping
29 reductions, irrigation practices

30
31 **Key Points:**

- 32 ● The long-term effectiveness of groundwater conservation initiatives based on pumping
33 reductions is dependent on lagged processes
- 34 ● Vertical hydraulic conductivity (K_z) controls if lagged responses are lateral-flow
35 dominated or recharge-dominated
- 36 ● In our model, failure to account for lagged processes overestimates the median usable
37 lifetime by 32 (lateral-flow-dominated) or 133 years (recharge-dominated)
- 38

39 **Abstract**

40 Many irrigated agricultural areas seek to prolong the lifetime of their groundwater
41 resources by reducing pumping. However, it is unclear how lagged responses, such as reduced
42 groundwater recharge caused by more efficient irrigation, may impact the long-term
43 effectiveness of conservation initiatives. Here, we use a variably saturated groundwater model to:
44 1) analyze aquifer responses to pumping reductions, 2) quantify time lags between reductions
45 and water level responses, and 3) identify the physical controls on lagged responses. We explore
46 a range of plausible model parameters for an area of the High Plains Aquifer (USA) where
47 stakeholder-driven conservation has slowed groundwater depletion. We identify two types of
48 lagged responses that reduce the long-term effectiveness of groundwater conservation, recharge-
49 dominated and lateral-flow-dominated responses, with vertical hydraulic conductivity (K_z)
50 dictating which response is dominant. When high K_z allows percolation to reach the aquifer,
51 more efficient irrigation reduces groundwater recharge. By contrast, when low K_z impedes
52 vertical flow, short term changes in recharge are negligible, but pumping reductions alter the
53 lateral flow between the groundwater conservation area and the surrounding regions (lateral-
54 flow-dominated response). For the modeled area, we found that a pumping reduction of 30%
55 resulted in median usable lifetime extensions of 20 or 25 years, depending on the dominant
56 lagged response mechanism (recharge- vs. lateral-flow-dominated). These estimates are far
57 shorter than estimates that do not account for lagged responses. Results indicate that
58 conservation-based pumping reductions can extend aquifer lifetimes, but lagged responses can
59 create a sizable difference between initial perceived and long-term actual effectiveness.

60 **1. Introduction**

61 Irrigation uses the majority (69%) of fresh groundwater withdrawals in the United States
62 (DeSimone et al., 2015; Dieter et al., 2018). In many aquifers supporting irrigated agriculture,
63 heavy pumping has resulted in unsustainable water-level declines, threatening the economy and
64 environment (Huggins et al., 2022; Deines et al., 2020; Scanlon et al., 2012). As groundwater is
65 a limited resource, how to mitigate these declines to extend the usable lifetime of heavily
66 stressed aquifers is a pressing question (Bierkens & Wada, 2019; Butler et al., 2020a; Castilla-
67 Rho et al., 2019; Gleeson et al., 2020). In semi-arid environments with little access to surface
68 water, groundwater conservation programs that seek to reduce pumping are one of the only
69 viable options to decrease groundwater declines in the near to moderate term (Butler et al.,
70 2020b; Deines et al., 2019; Hu et al., 2010).

71 The fundamental premise of groundwater conservation is to reduce outflows from the
72 aquifer by reducing pumping. However, it is not clear how the effectiveness of such conservation
73 initiatives might change in the future as the hydrological system in areas with groundwater
74 conservation adjusts to the observed pumping reductions (Butler et al., 2020b; Deines et al.,
75 2021; Foster et al., 2017). For example, the transit time for water at the land surface to percolate
76 downward and become groundwater recharge can vary dramatically over the High Plains aquifer
77 due to variations in unsaturated zone thickness and vertical hydraulic conductivity (K_z), with
78 estimates ranging from decades to centuries (Gurdak et al., 2008; Katz et al., 2016; McMahon et
79 al., 2006; Zell & Sanford, 2020). Current management approaches are often implemented with a
80 time horizon of years to decades (Miro & Famiglietti, 2019; Whittemore et al., 2018), while
81 effective groundwater sustainability requires setting and meeting long-term (multi-generational)
82 goals (Gleeson et al., 2012). Evaluating groundwater conservation programs on multi-decadal

83 timescales requires quantifying the long-term response of aquifer water levels to pumping
84 reductions.

85 The aquifer response to changes in pumping is a function of the pumping and a quantity
86 termed net inflow, which is defined as total inflows (i.e., recharge, lateral inflows) minus all non-
87 pumping outflows (i.e., discharge to streams, vegetation, lateral outflows), and is mediated by
88 hydrostratigraphic characteristics (Butler et al., 2016). However, the relative contributions of
89 vertical and lateral flows to net inflow are poorly understood and difficult to parse (Butler et al.,
90 2016, 2020b). While recent work has found that reductions in aquifer net inflow can decrease the
91 effectiveness of groundwater conservation programs over time (Butler et al., 2020b), the
92 mechanisms, timescales, and variations in magnitudes of lagged responses from different water
93 balance components is not known. As a result, we do not know which lagged responses may
94 impact overall groundwater sustainability, nor the timescales and controlling processes.

95 To address this knowledge gap, we seek to answer the question: *How do lagged*
96 *responses to pumping reductions impact the effectiveness of groundwater conservation practices*
97 *over time?* We hypothesize that when groundwater conservation initiatives, such as Kansas'
98 LEMA program, are enacted, (i) the reduction in pumping causes an immediate change to the
99 aquifer water balance, leading to a slowing of the water table decline rate (Figure 1, light blue
100 line); (ii) over time, inflows will diminish because the reduction in deep percolation (water that
101 drains below the rooting zone) associated with more efficient irrigation (Deines et al., 2021) will
102 eventually reduce recharge to the aquifer. Similarly, lateral inflow to the conservation area will
103 diminish, as decreased pumping will reduce the hydraulic gradient driving water into the area. In
104 both situations, the result will be an increase in water table declines to an intermediate rate

105 between the pre-conservation decline rate and the immediate post-conservation rate (dark blue
106 line in Figure 1).

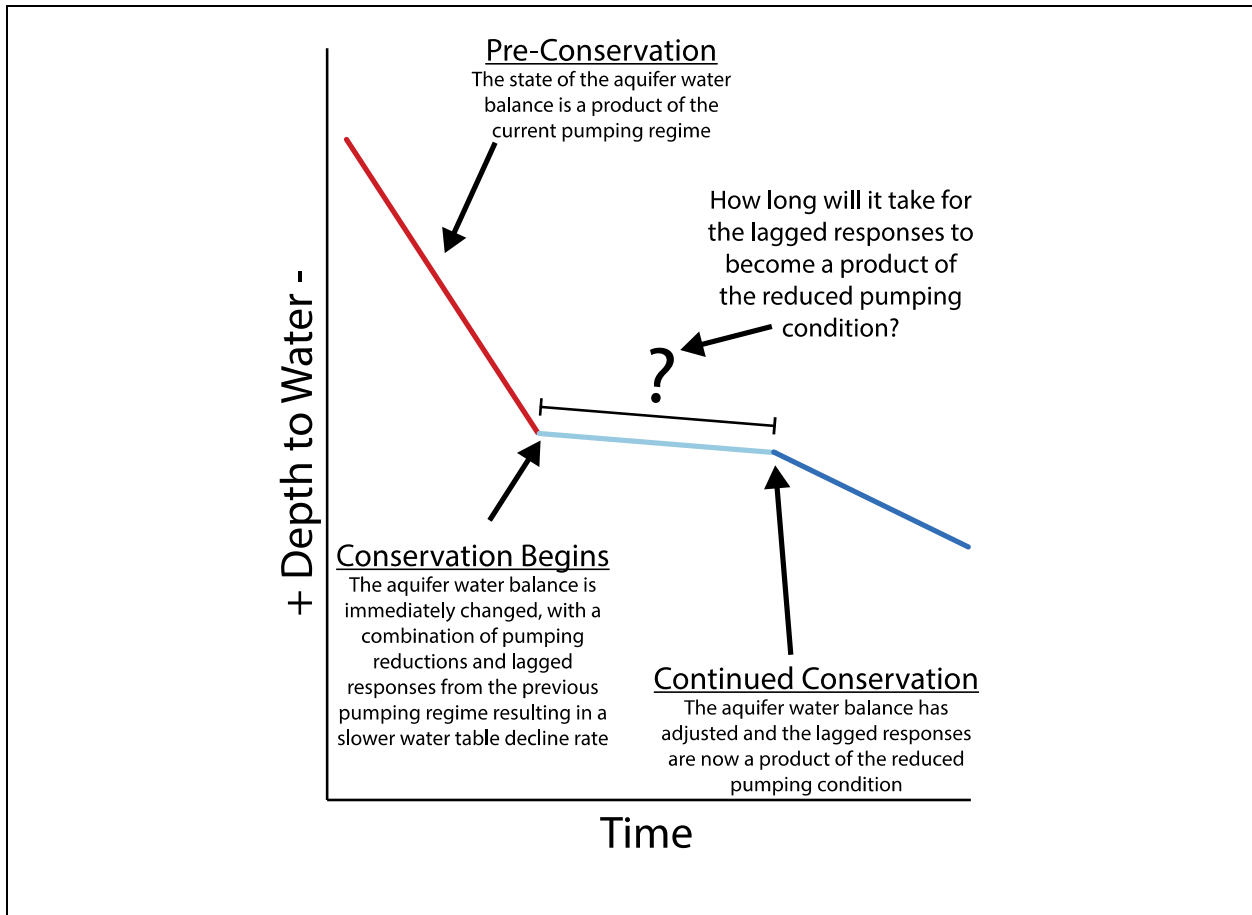


Figure 1: Graphical representation of hypothesized aquifer water balance changes due to pumping reductions. The initial reduction in pumping causes an immediate change to the aquifer water balance, resulting from an initial period of high effectiveness (light blue line) that wanes in time as lagged responses, such as groundwater recharge and lateral flow, adjust to the new pumping regime (dark blue line).

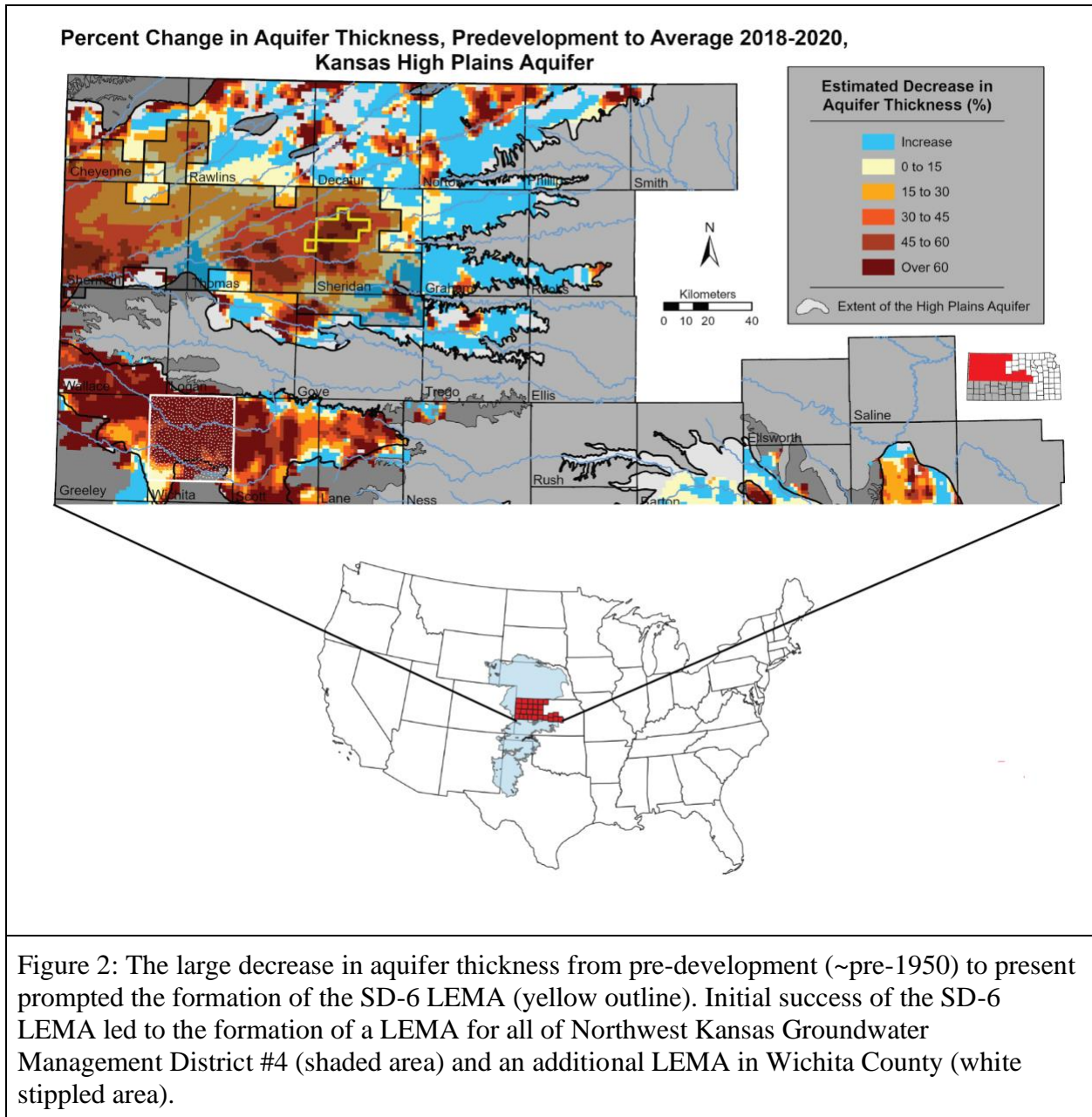
107 To test these hypotheses, we developed a variably saturated groundwater flow model for
108 the SD-6 LEMA based on historical observations and realistic conditions. To ensure that results
109 were not reflective of site-specific phenomena we employed a simplified surrogate modeling
110 approach. We used this model to evaluate the long-term changes in the aquifer water balance
111 associated with groundwater conservation, quantify the implications of lagged responses for

112 estimates of usable aquifer lifetimes, and determine the physical controls on these lagged
113 responses.

114 **2. Methods**

115 ***2.1 Study region***

116 We used the Sheridan-6 Local Enhanced Management Area (SD-6 LEMA) in Kansas as
117 a representative groundwater conservation program to evaluate these hypotheses. Located within
118 the portion of the High Plains aquifer in northwestern Kansas, the SD-6 LEMA overlies a thick
119 section of highly transmissive, unconsolidated sediments. There are no sources of surface water
120 in the region and therefore groundwater is heavily pumped to support irrigated agriculture
121 (Whittemore et al., 2018). LEMAs are a stakeholder-driven governance approach in which
122 groundwater users (primarily irrigators) and groundwater management districts develop
123 conservation plans; such plans have been implemented in several areas of Kansas over the past
124 decade (Figure 2). Once approved by the state, LEMAs are enforced by the state regulatory
125 agency (Kansas Statutes Annotated 82a-1041, 2012). SD-6, the state's first LEMA, was initiated
126 in 2013 in a 255-km² area in northwest Kansas with the stated goal of reducing annual pumping
127 by 20% over a five-year period. During that period, irrigators exceeded their goal, reducing
128 pumping by 31% on average and slowing water table decline rates while maintaining similar
129 economic returns (Deines et al., 2019, 2021; Golden, 2018; Whittemore et al., 2018). This initial
130 success led to an extension of the SD-6 LEMA for an additional five years, the 2018 formation
131 of a much larger LEMA that encompasses most of the northwest Kansas portion of the High
132 Plains aquifer (Northwest Kansas Groundwater Management District #4), and an additional
133 2021-initiated LEMA in west-central Kansas (Kansas Department of Agriculture, 2013, 2018,
134 2021) (Figure 2).



135

136 **2.2 Model Overview**

137 To test our hypotheses, we developed a variably saturated groundwater flow model of an
 138 arbitrary north-south linear transect that passes through the SD-6 LEMA (Figure 3). We elected
 139 to build a simplified model, rather than a fully-calibrated three-dimensional groundwater flow
 140 model, to better isolate the hydrological processes of interest, and more directly test our

141 hypotheses by avoiding unnecessary site-specific complexity--an approach known as surrogate
142 or archetypal modeling (Asher et al., 2015; Razavi et al., 2012; Voss, 2011a, 2011b; Zipper et
143 al., 2018, 2019). Nevertheless, to ensure our model provided a reasonable simulation of the
144 dominant processes in this region, we conducted an evaluation against field data from the SD-6
145 region, and conducted a sensitivity analysis to test the impact of simplifying assumptions on
146 model results.

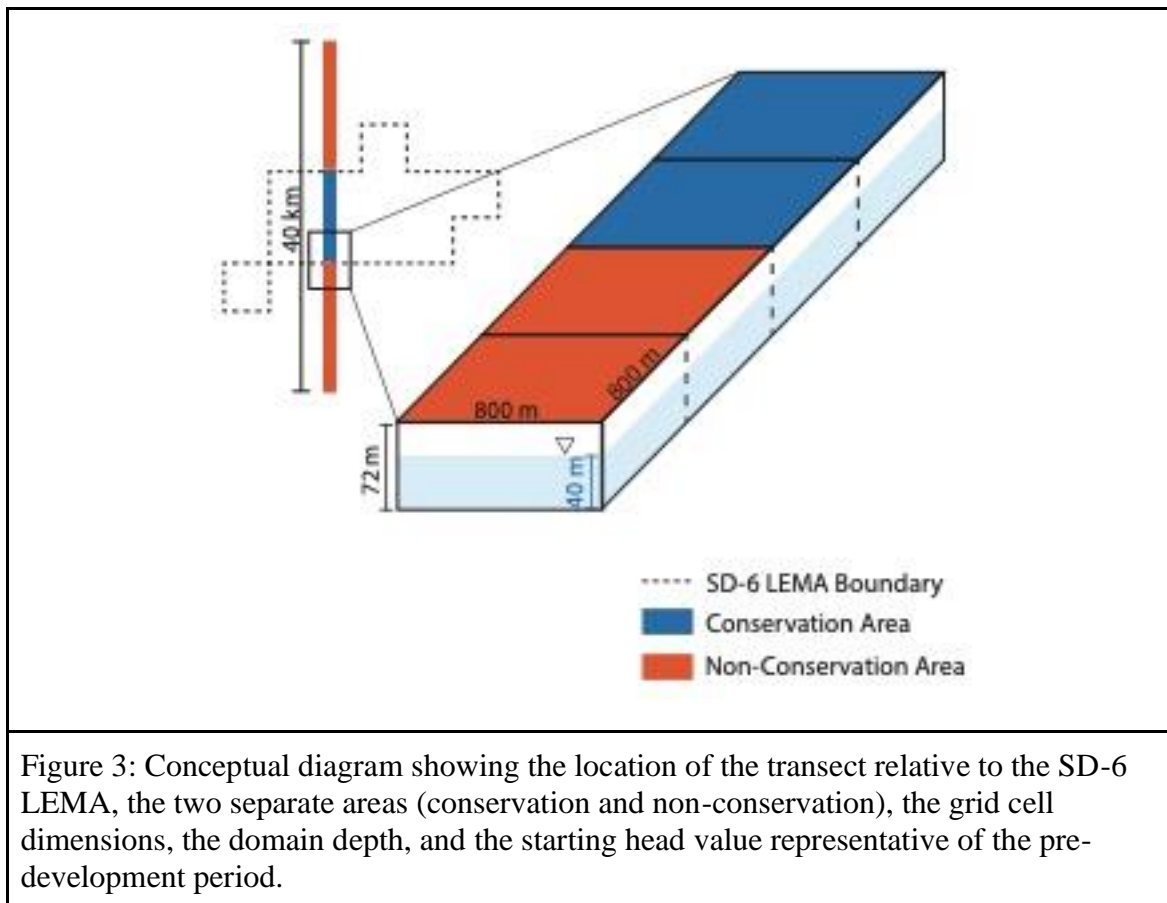


Figure 3: Conceptual diagram showing the location of the transect relative to the SD-6 LEMA, the two separate areas (conservation and non-conservation), the grid cell dimensions, the domain depth, and the starting head value representative of the pre-development period.

147

148 **2.3 Model Construction and Input Data**

149 We used the United States Geological Survey's MODFLOW-NWT program and
150 constructed the model using the Python package FloPy (Bakker et al., 2016). The 40 km long
151 domain consists of a single layer of 50 grid cells, each 800 m by 800 m in size, covering a total

152 area of 32 km². Each grid cell is roughly equivalent in area to a typical field size in the region
153 (64.75 hectares [160 acres]) and cell dimensions were set based on the typical distance between
154 irrigation wells in the area (Figure S1). The model domain was split into two types of
155 management practices (conservation and non-conservation; blue and orange areas, respectively,
156 in Figure 2b), which were represented in the model using different pumping and deep percolation
157 rates as described below. The conservation area was made up of 14 grid cells while the non-
158 conservation areas each consisted of 18 grid cells, with the four additional cells being added to
159 remove the influence of edge effects from the northern and southern no-flow boundaries. The
160 single model layer is 72 m thick and starting pressure heads were set to 40 m; these values
161 represent the average depth to bedrock and pressure heads, respectively, of the area for the pre-
162 development period (~pre-1950) (Fross et al., 2012). The top of the model is assumed to be
163 below the rooting zone to remove the influence of evapotranspiration, overland flow, and
164 discharge to surface water bodies. Regional groundwater flow is perpendicular to our transect
165 from west to east (Fross et al., 2012, Figure S2), so we included a lateral flow boundary
166 condition on the west side and a no-flow boundary on the east to represent the net lateral flow
167 entering the modeled area, which is distinct from the vertical inflow from groundwater recharge.
168 Since our model is a two-dimensional transect, this approach reduces the number of uncertain
169 parameters by lumping inflow from the west and outflow to the east into a single net lateral
170 inflow term. We varied net lateral flows along with the model hydrostratigraphic properties as
171 described in Section 2.3.

172 Pumping and deep percolation rate time series were developed using a combination of
173 historical annual precipitation depth, regression model-based historical pumping data (1955-
174 1992) (Wilson et al., 2005), and measured pumping volumes (1993-2018). We estimated annual

175 pumping volumes by establishing relationships between annual areally averaged precipitation
176 depth and applied irrigation depth during the 2000-2018 period (Figure 4), the period after a
177 large majority of irrigators had transitioned from traditional high pressure center pivot irrigation
178 to more efficient center pivot with drop nozzle irrigation (Pfeiffer & Lin, 2010; Rogers & Lamm,
179 2012). We first estimated annual areally averaged applied irrigation depth as the total pumping
180 volume from wells within SD-6 divided by the total area. Observed pumping rates from the SD-6
181 LEMA were translated upward to account for the climate-adjusted 27% reduction in pumped
182 volume observed during the first four years of the LEMA (Whittemore et al., 2018). We then
183 developed a relationship between precipitation and irrigation depth for the “No Conservation”
184 portions of the domain that included the period after the establishment of the SD-6 LEMA
185 (2000-2018). We developed two additional relationships to simulate practices by modifying the
186 “No Conservation” relationship (Figure 4a): (i) a 20% pumping reduction scenario based on the
187 legal requirements for the SD-6 LEMA; and (ii) a 30% pumping reduction scenario that more
188 closely reflects observed irrigator behavior.

189 For each pumping scenario, we then calculated the applied pumping volume for each grid
190 cell as the product of irrigation depth from the statistical relationship (Figure 4a) and the area of
191 the grid cell. We disaggregated the estimated annual pumping volume uniformly over a 103-day
192 period, which was the average time between the onset and cessation of irrigation pumping in the
193 region interpreted from high temporal-resolution well observations (Butler et al., 2019)..
194 Pumping is simulated using MODFLOW’s well (WEL) package. As discussed in Section 2.2,
195 our surrogate modeling approach is not intended to precisely represent observed spatial pumping
196 dynamics within the SD-6 LEMA, but rather the average aquifer response to typical regional
197 pumping. To reflect that the estimated pumping volume is representative of the entire SD-6 area,

198 which is heavily irrigated, we placed a pumping well in each individual grid cell both inside and
199 outside the conservation area. Due to the small amount of north-south variation in precipitation
200 in our study domain (Figure S3), we used the same precipitation for estimating pumping in all
201 grid cells so pumping was uniform within the conservation and non-conservation areas.

202 The model simulates flow through variably saturated porous media using the unsaturated
203 zone flow (UZF) package, which uses a kinematic-wave approximation to solve the 1-D
204 Richard's equation (Niswonger et al., 2006; Smith, 1983; Smith & Hebbert, 1983). While
205 numerous models can simulate variably saturated flow, the UZF package for MODFLOW has
206 several advantages for our purposes, including documented applications in thick vadose zones
207 (Hunt et al., 2008; Nazarieh et al., 2018), computational efficiency (Kennedy et al., 2016;
208 Niswonger & Prudic, 2009), and widespread use (Bailey et al., 2013; Hou et al., 2020; Morway
209 et al., 2013). Since the top of our model domain represents the bottom of the root zone, we
210 provided UZF with annual values of deep percolation from a linear model fit between simulated
211 deep percolation from a calibrated crop model for the SD-6 area with and without conservation
212 (Deines et al., 2021), and the sum of annual precipitation and applied irrigation depth following
213 Scanlon et al. (2006) (Figure 4b). Like pumping, annual deep percolation values were uniformly
214 disaggregated to daily values over the 103-day pumping period. This assumption is justified
215 because our deep percolation estimates are based on the SALUS model which simulates the root
216 zone water balance including precipitation, irrigation, evaporation, and root water uptake (Deines
217 et al., 2021). Unlike the separate relationships required for pumping under each conservation
218 scenario, only one relationship is needed to estimate deep percolation because the effects of
219 groundwater conservation are accounted for in the annual irrigation depth term. These
220 relationships (Figures 4a and 4b) were used to generate deep percolation rate time series for both

221 the evaluation and projection periods as well as pumping rate time series for the projection
222 period (Figure 4c). Pumping rate time series for the evaluation period were generated using a
223 combination of regression model-based and measured pumping rates.

224

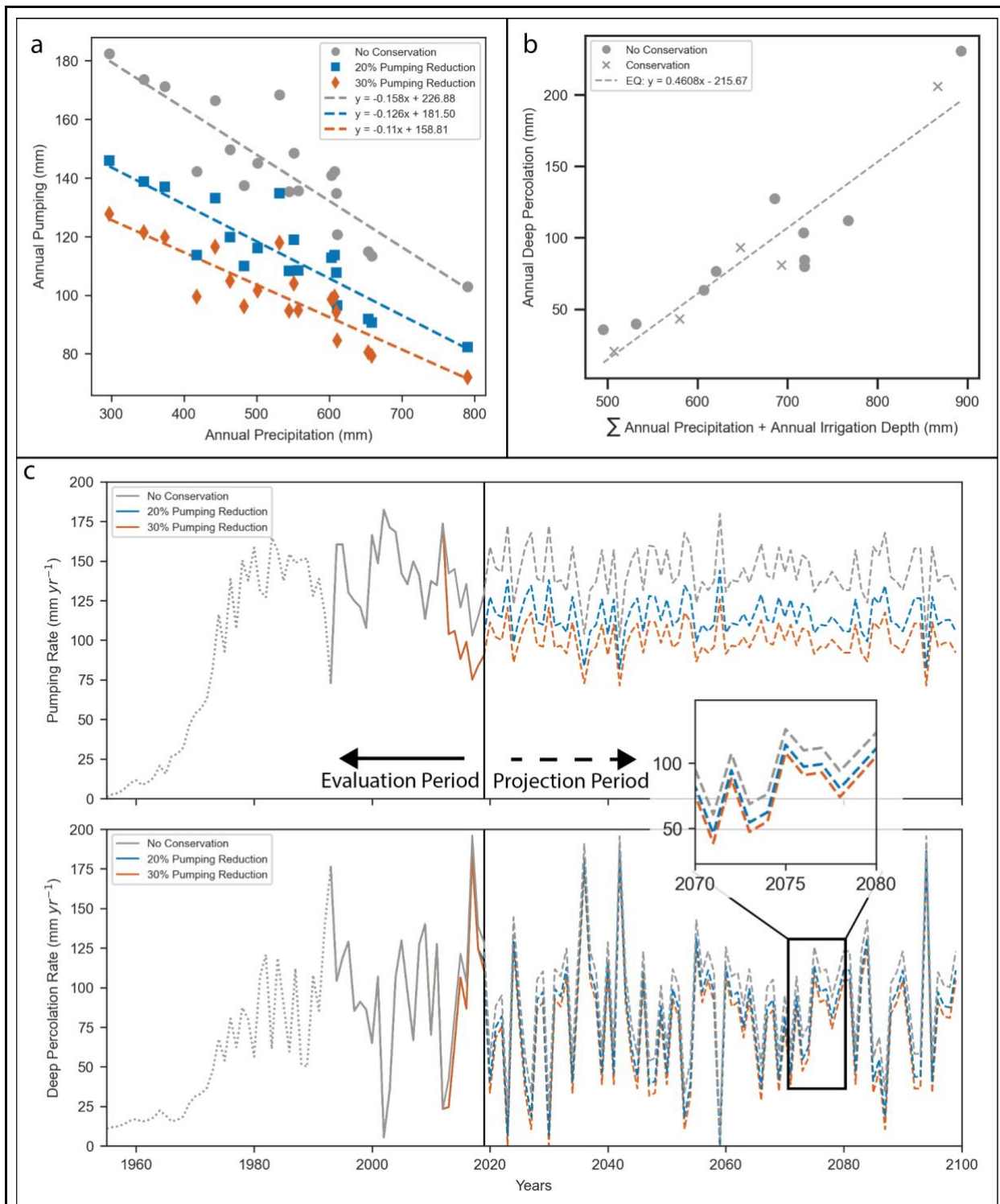


Figure 4: Annual statistical relationships for: a) pumping depth, b) deep percolation depth, and resulting applied c) pumping rate and d) deep percolation from the statistical relationships. For three very dry years in the prediction period, the statistical relationship in panel b produced negative deep percolation rates; these years were assigned a rate of 0 m d^{-1} . For the historical

period, pumping rate and deep percolation are shown only for the 30% pumping reduction scenario (orange) as this best represents observed irrigator behavior.

225

226 Our simulations spanned 201 years (1900-2100), which can be divided into three periods:

227 spin-up (1900-1954), historical (1955-2019), and projection (2020-2100). The 55-year spin-up

228 period is prior to the onset of high capacity pumping in the region so the only fluxes in/out of the

229 domain are deep percolation, which was applied at a rate of $5 \times 10^{-4} \text{ m d}^{-1}$ (51.5 mm yr⁻¹) to

230 approximate pre-development recharge in the area (Fross et al., 2012; Hansen, 1991), and the

231 applied lateral inflows. To ensure that recharge and lateral inflow did not change the prescribed

232 pre-development saturated zone pressure heads, a drain was placed at the pre-development water

233 level (40 m) across the domain. This approximates the effect of the regional streams that drained

234 the system during the pre-development period. After the spin up period, a mix of regression-

235 estimated (1955 to 1992) (Wilson et al., 2005) and measured pumping volumes (1993 to 2018)

236 for the SD-6 area was used to generate normalized pumping rates which were applied to the

237 model (Figure 4c). Pumping data for the year 2019 was estimated using the statistical regression

238 as pumping data was not available, but this year was included in the evaluation period as water

239 level change and head data were available at the time of model development. As observed

240 irrigator behavior within the LEMA was close to the 30% pumping reduction scenario, we used

241 the 30% reduction pumping rates for 2013-2019. The projection period (2020-2100) allows us to

242 evaluate the long-term implications of pumping with the baseline and the two reduction (20%

243 and 30%) pumping scenarios. For the projection period, we randomly sampled annual

244 precipitation from the historical precipitation record to estimate pumping and deep percolation

245 for each year based on the relationships shown in Figure 4 since there are no consistent long-

246 term historical (Lin et al., 2017) or projected (Figure S4) precipitation trends in this region, and

247 historical precipitation patterns do not exhibit significant temporal autocorrelation (Butler et al.,
248 2020b).

249 **2.4 Model Evaluation and Evaluation of Control Parameters**

250 We used a Latin hypercube sampling scheme (McKay et al., 1979) to identify the model
251 parameters that best reproduced observed hydrological data, and evaluate the sensitivity of
252 model output to each parameter and the interactions between parameters (Zipper et al., 2018).
253 Our Latin hypercube sample consisted of 2,000 near-random, unique sets of hydrostratigraphic
254 parameters (vertical saturated hydraulic conductivity, K_z ; specific yield, S_y ; Brooks and Corey
255 epsilon, ϵ) and lateral inflow (LI), which were selected from a uniform distribution over the
256 parameter space shown in Table 1. We ran one simulation using each parameter set to explore
257 lagged responses to groundwater conservation across a range of hydrogeological settings and to
258 reduce the risk of identifying a local optima as the best parameter set.

Table 1: Parameter space ranges for the Latin hypercube sampling scheme. As we are taking a surrogate modeling approach, ranges were extended outside of their observed values for the area to allow the parameter space to be fully explored. ¹(Fross et al., 2012) ²(Butler et al., 2016), ³(Brooks & Corey, 1966)

Parameter	Lower Bound	Upper Bound
\log_{10} Vertical Hydraulic Conductivity (m d^{-1})^[1]	-6	1
Specific Yield (-)^[2]	0.06	0.18
Brooks and Corey Epsilon (-)^[3]	2	5
\log_{10} Lateral Inflows (m d^{-1})^[2]	-6	-3

259

260 Horizontal hydraulic conductivity and saturated water content were held constant at 20 m
261 d^{-1} and 0.25, respectively, to reflect average values in the SD-6 LEMA area (Fross et al., 2012).
262 The UZF package relies on the Brooks and Corey function to calculate unsaturated K_z (Brooks
263 & Corey, 1966). This function requires residual water content, here approximated for each
264 parameter set by taking the S_Y value for each set and subtracting it from the saturated water
265 content (Niswonger et al., 2006). A value of 0.005 was added to the calculated residual water
266 content to ensure that the unsaturated hydraulic conductivity value did not start at a value of
267 zero.

268 We evaluated the performance of each of the 2000 simulations via comparison to the
269 observed groundwater level data for the 1999-2019 period, which represents the longest
270 continuous record of reliable observations within the SD-6 LEMA (KGS WIZARD Database;
271 <http://www.kgs.ku.edu/Magellan/WaterLevels/index.html>). The goal of this study is to ensure
272 that the dominant processes (e.g., pumping reductions and lagged responses) are appropriately
273 simulated while not overparameterizing the model since our focus is not on site-specific
274 heterogeneity (Konikow & Bredehoeft, 1992).

275 We quantified model performance for each parameter set using a two-step approach.
276 First, as the area has experienced significant drawdown, we eliminated model runs in which the
277 head in the model domain at the end of the historical period (2019) was still at or above pre-
278 development levels (Fross et al., 2012). For the remaining runs, we calculated the Kling-Gupta
279 Efficiency (KGE; Kling et al., 2012) score for both the annual water table elevation and the
280 interannual change in water table elevation, which are based on measurements taken each
281 January in the LEMA area. We selected these two metrics to ensure that both the long-term and
282 interannual dynamics were simulated reasonably, and used the minimum (lower-performing) of

283 these two KGE values as the final KGE score for that parameter set. We then divided the model
284 runs into four performance groups: poor ($KGE < -0.41$, which indicates that the model results are
285 worse than the mean of the observations; Knoben et al., 2019), low ($-0.41 < KGE < 0$), medium
286 ($0 < KGE < 0.5$), and high ($KGE > 0.5$). A KGE score of 1 would indicate a perfect match
287 between a simulation and observations. Only runs in the high performance group were analyzed
288 for the projection period because those parameter sets were able to reasonably approximate
289 historical hydrological conditions. We also conducted a sensitivity analysis to determine the
290 influence of several simplifying assumptions (model discretization, model homogeneity, uniform
291 distribution of pumping wells) on model results. To do this, we ran five additional model
292 scenarios with a smaller grid cell dimension in which each simplification was analyzed further
293 (see Supplemental Information for details).

294 The models selected for projection were run to the year 2100 and the extension of the
295 usable aquifer lifetime was quantified for the 20% and 30% pumping reduction scenarios. For
296 each parameter combination and pumping scenario, the extension of the usable aquifer lifetime is
297 calculated as the number of years that water levels in the aquifer remain above a minimum
298 threshold relative to the baseline “No Conservation” scenario. For this region, we assumed that a
299 minimum saturated thickness of eight meters is required for large-scale irrigation to allow for
300 sufficient transmissivity, and therefore well yield, along with pumping-induced drawdown in the
301 well (Deines et al., 2020; Butler et al., 2020b).

302

303 **3. Results and Discussion**

304 **3.1 Recharge and lateral flow-dominated inflows**

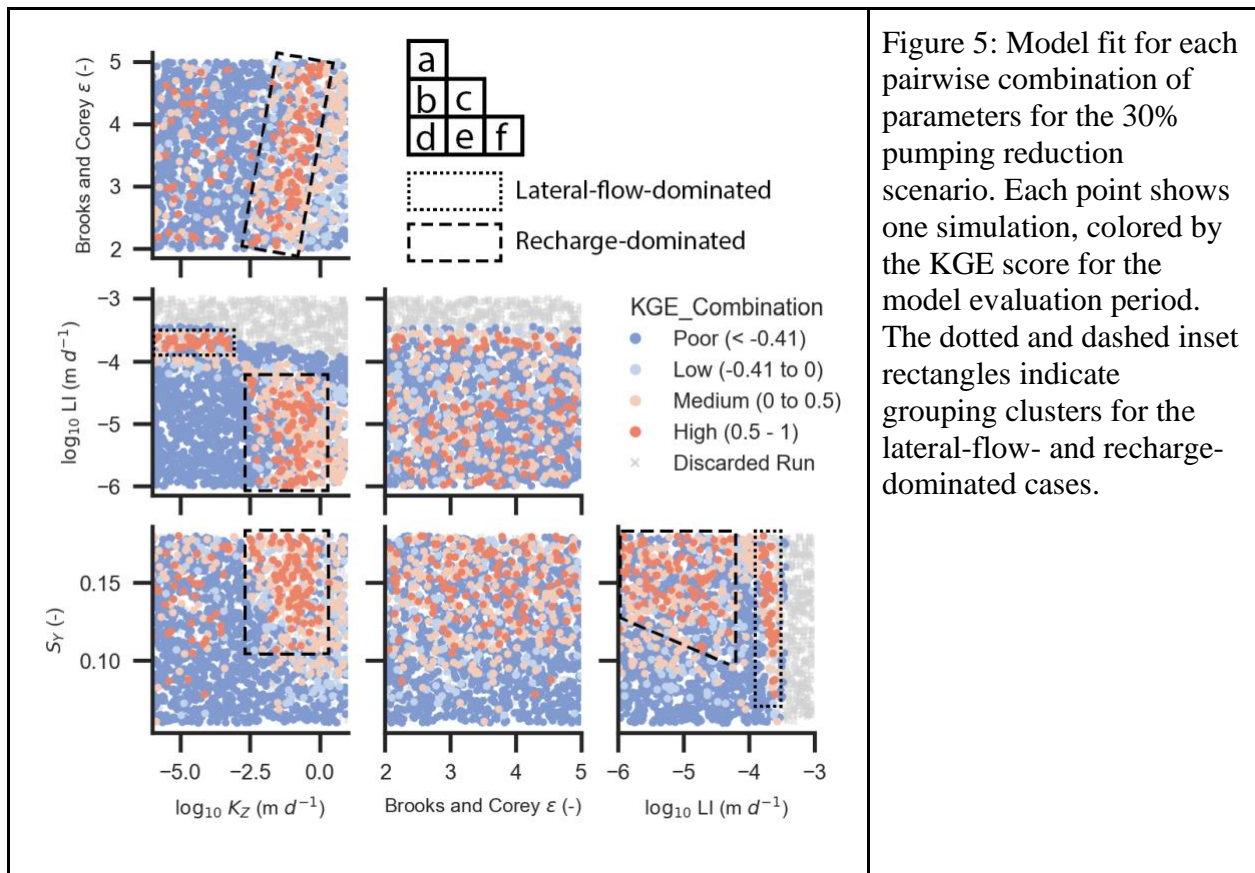


Figure 5: Model fit for each pairwise combination of parameters for the 30% pumping reduction scenario. Each point shows one simulation, colored by the KGE score for the model evaluation period. The dotted and dashed inset rectangles indicate grouping clusters for the lateral-flow- and recharge-dominated cases.

305 We found that many parameter combinations were able to reproduce the historical head
306 and head change observations (Figure 5). Of the 2,000 parameter combinations tested, there were
307 122 simulations rated as high performance (Figure 5, dark red circles, $KGE > 0.5$). An additional
308 214 were rated as medium, 126 as low, 1,090 as poor, and 448 were discarded due to no
309 simulated drawdown (Figure 5). Within parameter pairs, there are several clusters that occur
310 throughout the parameter space (Figure 5b), the most evident occurring between lateral inflow
311 (LI) and vertical hydraulic conductivity (K_z). In parameter space, these two clusters correspond
312 to a high LI/low K_z zone, in which lateral groundwater flow is the dominant inflow to the
313 aquifer, and a low LI/high K_z zone, in which vertical groundwater recharge is the dominant
314 inflow to the aquifer.

315 For the lateral-flow-dominated case, the parameter sets that yield high KGE scores have
316 LI values between 1.6×10^{-4} and $2.5 \times 10^{-4} \text{ m d}^{-1}$ and K_Z values between 1×10^{-6} (the lower
317 bound of the parameter space tested) and $5 \times 10^{-4} \text{ m d}^{-1}$. However, for the Brooks and Corey ϵ
318 and S_Y there are no clear thresholds, indicating that the rate of lateral flow is the controlling
319 factor. The ranges of K_Z and LI values with good fits in the recharge-dominated case are
320 opposite of the lateral-flow-dominated case, with higher K_Z values (from 3.5×10^{-3} to 1 m d^{-1})
321 and lower LI values (from $5 \times 10^{-5} \text{ m d}^{-1}$ to the lower bound of the parameter space tested, 1×10^{-6}
322 m d^{-1}) (Figure 5b). In contrast to the lateral-flow-dominated case, the recharge-dominated case
323 is also sensitive to the Brooks and Corey ϵ and S_Y . As K_Z approaches 1 m d^{-1} , the value of ϵ
324 steadily increases from 2 to 5 (Figure 5a). The range of S_Y is also limited based on K_Z , with S_Y
325 values between 0.1 and 0.18 necessary to generate KGE scores of ≥ 0.5 (Figure 5d). Vertical
326 hydraulic conductivity is not the only controlling factor in the recharge-dominated case. As the
327 value of LI increases towards its upper limit of $5 \times 10^{-5} \text{ m d}^{-1}$, the range of S_Y also expands with
328 its lower limit dropping from 0.13 to 0.1 (Figure 5f). The interplay between hydrostratigraphic
329 parameters plays a more prominent role in the recharge-dominated scenario. Along with K_Z , the
330 Brooks and Corey ϵ and S_Y influence the rate and volume of vertical water movement through
331 the thick vadose zone, respectively, and therefore influence the performance of the model.

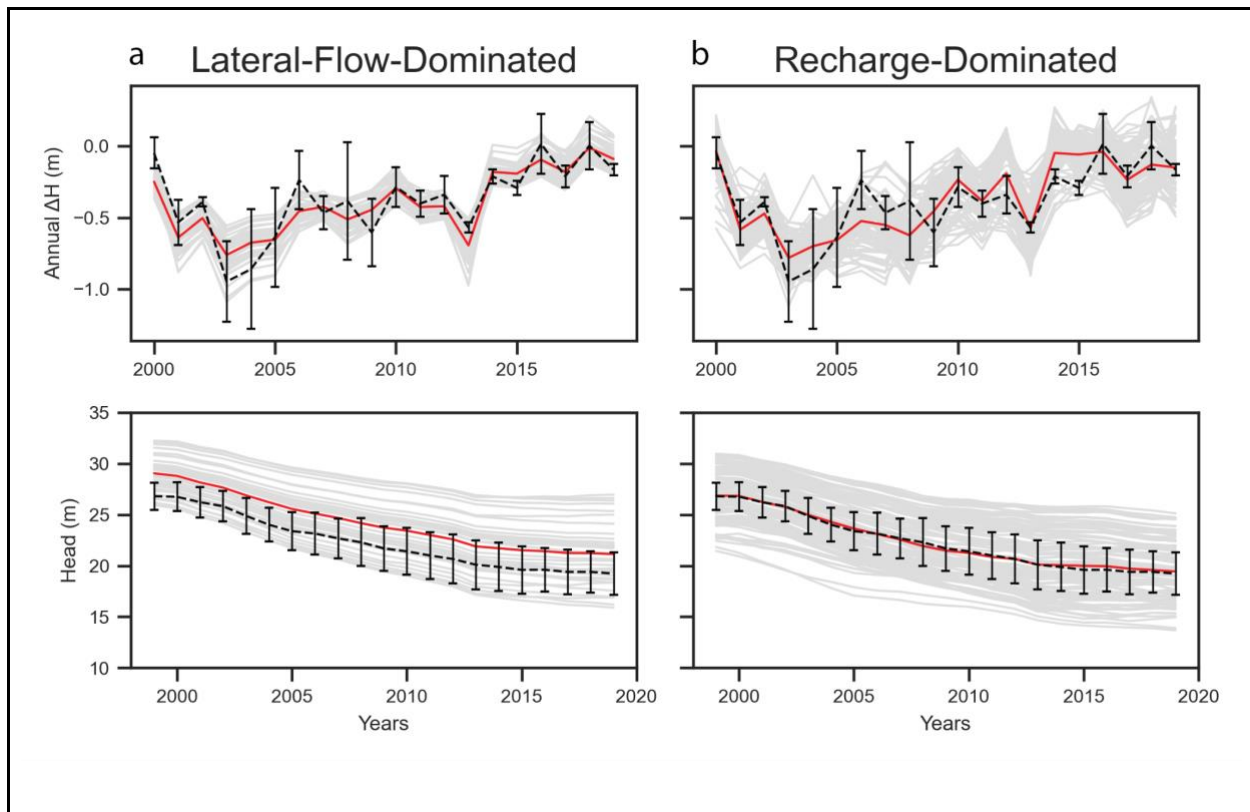


Figure 6: Results for the 30% pumping reduction scenario of observed (black, dashed line), simulated (light gray, solid lines), and average simulated (red lines) interannual change in pressure head and annual pressure head values for the a) lateral-flow-dominated and b) recharge-dominated cases. Simulation results presented for the center cell in the conservation area, the error bars show one standard deviation about the mean of the observed data.

332

333 For both the lateral-flow-dominated and recharge-dominated cases, the average simulated

334 interannual change in pressure head and annual pressure head values (Figure 6a, b, red lines)

335 closely align to the average observed value (Figure 6a, b, dashed lines). The average KGE score

336 and root mean square error (RMSE) were quantified for all high-performing lateral-flow- and

337 recharge-dominated runs. In the lateral-flow-dominated cases the KGE score and RMSE for the

338 interannual change in head are 0.687 and 0.142 m, respectively. For the annual head, these

339 values are 0.776 and 2.226 m, respectively. In the recharge-dominated cases the KGE score and

340 RMSE for the interannual change in head are 0.644 and 0.205 m, respectively. For the annual

341 head, these values are 0.763 and 2.507 m, respectively. The average simulated values also fell

342 within or close to the standard deviation of the observed measurements, indicating that the model
343 is reasonably capturing the annual and interannual dynamics of the natural system. We also
344 tested the sensitivity of our model results to several of the simplifying assumptions adopted in
345 our surrogate modeling approach: model discretization, model homogeneity, uniform distribution
346 of pumping wells. We found that increasing the complexity of our model did not substantially
347 affect our results or interpretations (Figure S5, Table S1).

348 The wide variety of parameters that lead to reasonable agreement with the observed data
349 indicates that multiple interpretations of the underlying processes that dictate groundwater
350 recharge in areas with thick vadose zones are equally valid, following the principle of
351 equifinality (Beven, 2006). In groundwater modeling, parameter estimation often seeks to find a
352 local or global optimum to match limited observations while minimizing an objective function
353 using software such as PEST (Doherty, 2015) or UCODE (Poeter & Hill, 1999). However, the
354 hunt for an ideal parameter set that results in simulated values closely matching observed values
355 can ignore other possible parameter sets that perform nearly equally well (Savenije, 2001; Liu et
356 al., 2022). This is true for our surrogate model of the SD-6 area as the lack of vadose zone
357 observation data paired with an exploration of a wide parameter space resulted in two possible
358 and equally valid mechanisms that affect the long term performance of pumping reduction-based
359 groundwater conservation initiatives.

360 ***3.2 Lagged responses to conservation in recharge- and lateral flow-dominated conditions***

361 Recharge-dominated and lateral-flow-dominated cases exhibit different long-term
362 hydrological responses to groundwater conservation due to differences in lagged changes to the
363 aquifer water balance. In lateral-flow-dominated settings, changes in deep percolation caused by
364 pumping reductions do not significantly impact recharge rates within the 80-year projection

365 period because recharge rates are low to begin with and changes in deep percolation take a long
366 time to propagate down to the water table (Figure 7a). Following reductions in pumping, water
367 table decline rates undergo an initial dramatic reduction then increase through time, consistent
368 with our hypothesis (Figure 1). The increase occurs because the initial reduction within the
369 conservation area creates a lateral hydraulic gradient that drives lateral flow into the surrounding
370 non-conservation area; this phenomenon is further discussed in Section 3.3. In the lateral flow-
371 dominated case, high fluxes of net lateral inflow compensate for the lack of recharge. This case
372 only applies when K_z values are low as any increase in recharge would add too much water to
373 the aquifer, resulting in unrealistic rises in the water table. When LI is the controlling
374 mechanism, the Brooks and Corey ϵ has a negligible impact on the effectiveness of the pumping
375 reductions.

376 In recharge-dominated cases, deep percolation can travel through the unsaturated zone
377 rapidly enough that changes in irrigation depth can alter the rate of groundwater recharge within
378 our simulation period. Reductions in pumping decrease the amount of water that is applied in
379 excess of crop water demands, and thus reduce the rate of deep percolation (Figure 4b). Unlike
380 the lateral flow-dominated case where there is no difference in recharge between the
381 conservation and non-conservation areas over the time span of this analysis, the effects of
382 changing deep percolation led to a reduction in groundwater recharge within the conservation
383 area relative to the non-conservation area (Figure 7b). Once recharge decreases in response to the
384 reduced pumping condition, water table decline rates increase, consistent with our hypothesis
385 (Figure 1). However, even in recharge-dominated settings, conservation can lead to substantial
386 changes in transect-parallel lateral outflows. These lateral outflows across the border of the

387 conservation area reach up to $\sim 25 \text{ mm yr}^{-1}$, which is comparable to the difference in recharge
388 between the conservation and non-conservation areas (Figure 7b).

389

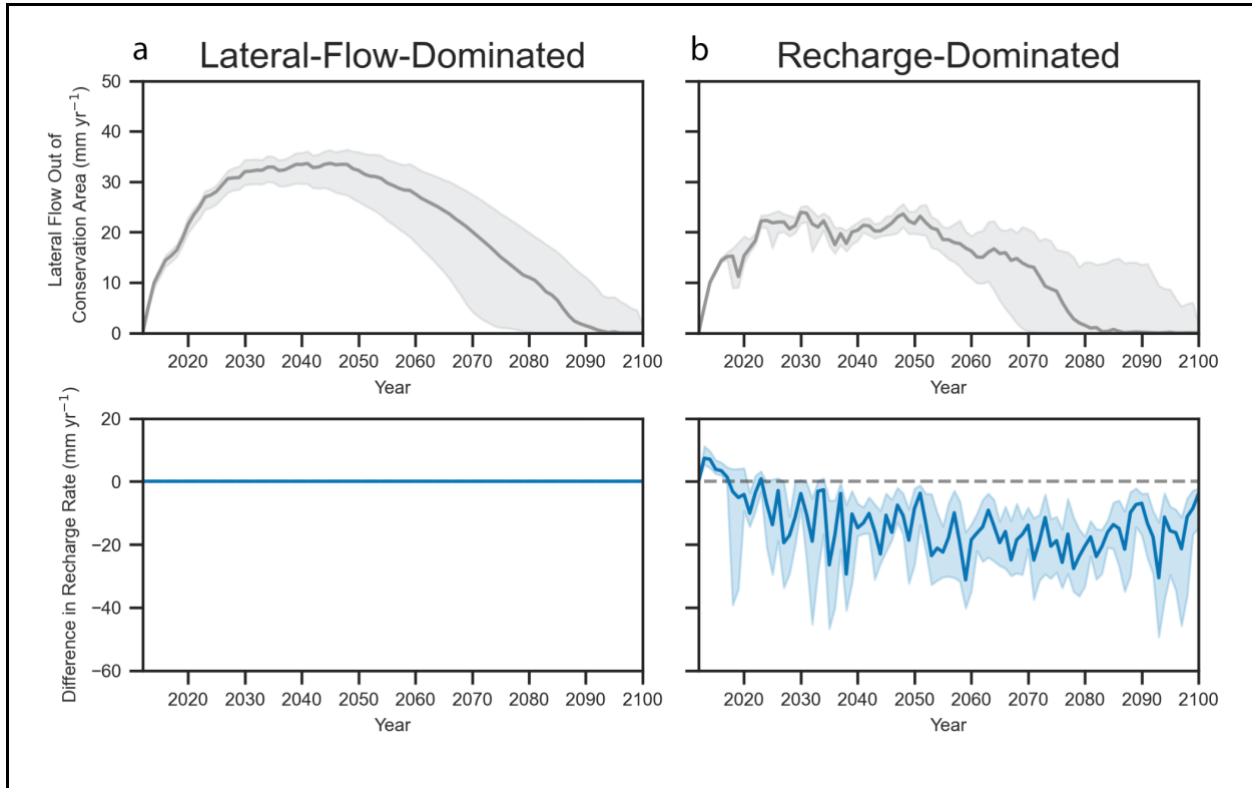


Figure 7: Average time series of simulated lateral outflow from the conservation area to the non-conservation area (gray lines, upper plots) and difference in recharge rate between the conservation area and the non-conservation area (blue lines, lower plots) for a) the lateral-flow-dominated and b) recharge-dominated cases. Thick lines represent average values across all model runs used for the projections and the shading indicates the interquartile range.

390

391 Lateral flow and recharge have distinct time lags from the onset of groundwater
392 conservation measures. For the lateral-flow-dominated cases, flow out of the conservation area
393 begins with the start of pumping reductions and increases quickly with the development of a
394 head gradient between the conservation and non-conservation areas. Eventually, lateral outflow
395 peaks at a rate of $\sim 34 \text{ mm yr}^{-1}$ from 2030 to 2050, or ~ 17 to ~ 37 years after the onset of
396 conservation (Figure 7a). After 2050, lateral outflow gradually decreases due to a decline in the

397 head gradient between the conservation and non-conservation areas, typically reaching 0 mm yr^{-1}
398 between 2080 and 2100 depending on the case. In the recharge-dominated cases (Figure 7b),
399 lateral flow out of the conservation area follows a similar pattern, though with a lower peak (~ 24
400 mm yr^{-1}) and more interannual variability. The interannual variability in lateral outflows in the
401 recharge-dominated cases is due to differences in recharge rates between the conservation and
402 non-conservation areas, with larger lateral outflows when the recharge differences between the
403 conservation and non-conservation areas are greater because this induces a larger hydraulic
404 gradient between the two areas. For the recharge-dominated cases, there is an immediate short
405 lived-period of positive differences in recharge rates, with recharge into the conservation area
406 greater than into the non-conservation area because the reduction in water table decline rates
407 allows more recharge to reach the water table than at higher decline rates. After five years,
408 recharge rates in the groundwater conservation area adjust to the lower deep percolation rates
409 associated with the reduced pumping condition, resulting in a negative difference for the rest of
410 the simulation.

411 These differences between the lateral- and recharge-dominated cases indicate that, in
412 settings with higher values of K_z (in our case, $> 0.0035 \text{ m d}^{-1}$; Figure 5), excess applied irrigation
413 water can traverse the thick vadose zone that is present in western Kansas and ultimately
414 recharge the water table. However, vertical hydraulic conductivity is not the only controlling
415 factor in the recharge-dominated cases, as LI , S_Y , and Brooks and Corey ϵ also play important
416 roles in the long-term effectiveness (see Figure 5). In cases where S_Y is low, high-performing
417 parameter sets tend to have a greater LI to compensate for the low drainable pore space. When
418 K_z values are low, Brooks and Corey ϵ values must be low as well to allow for the calculated
419 unsaturated hydraulic conductivity value to be high enough to transmit water through the vadose

420 zone at a rapid enough rate to initiate groundwater recharge. As K_z increases, so must the Brooks
421 and Corey ε , limiting the value of unsaturated hydraulic conductivity and preventing the aquifer
422 from becoming inundated with excess water.

423 ***3.3 Effects of lagged responses on aquifer usable lifetime***

424 These lagged responses to groundwater conservation led to different estimates of the
425 degree to which conservation extends the usable aquifer lifetime. The lateral-flow-dominated
426 cases had an average extension of 15 years for a 20% pumping reduction and an average
427 extension of 25 years for a 30% reduction (Figure 8a, c). Results were similar for the recharge-
428 dominated cases, where the average extension was 12 years with a reduction in pumping of 20%
429 and 20 years for a pumping reduction of 30% (Figure 8b, d). Using the start of the initial SD-6
430 LEMA in 2013, the remaining usable lifetime can be quantified. For the recharge-dominated
431 cases, if no pumping reductions are applied, the water table will fall below eight meters of
432 saturated thickness (the minimum thickness capable of supporting irrigated agriculture; Butler et
433 al., 2020b) in 2047. If pumping is reduced by 20% or 30%, the aquifer lifetime will be extended
434 to 2059 and 2067, respectively. For the lateral-flow-dominated cases, the water table will fall
435 below eight meters of saturated thickness in 2045 in the absence of pumping reductions. With a
436 20% and 30% pumping reduction, the lifetime is extended to 2060 and 2070, respectively. The
437 numbers found in this study are within the envelope found by Butler et al. (2020b) who used a
438 water balance approach to quantify the extension of usable lifetime under various exploratory
439 scenarios, but does not differentiate between lagged changes in recharge and lateral flow. Our
440 analysis extends this previous work by quantifying the relative importance of these two drivers
441 of long-term change in net inflows.

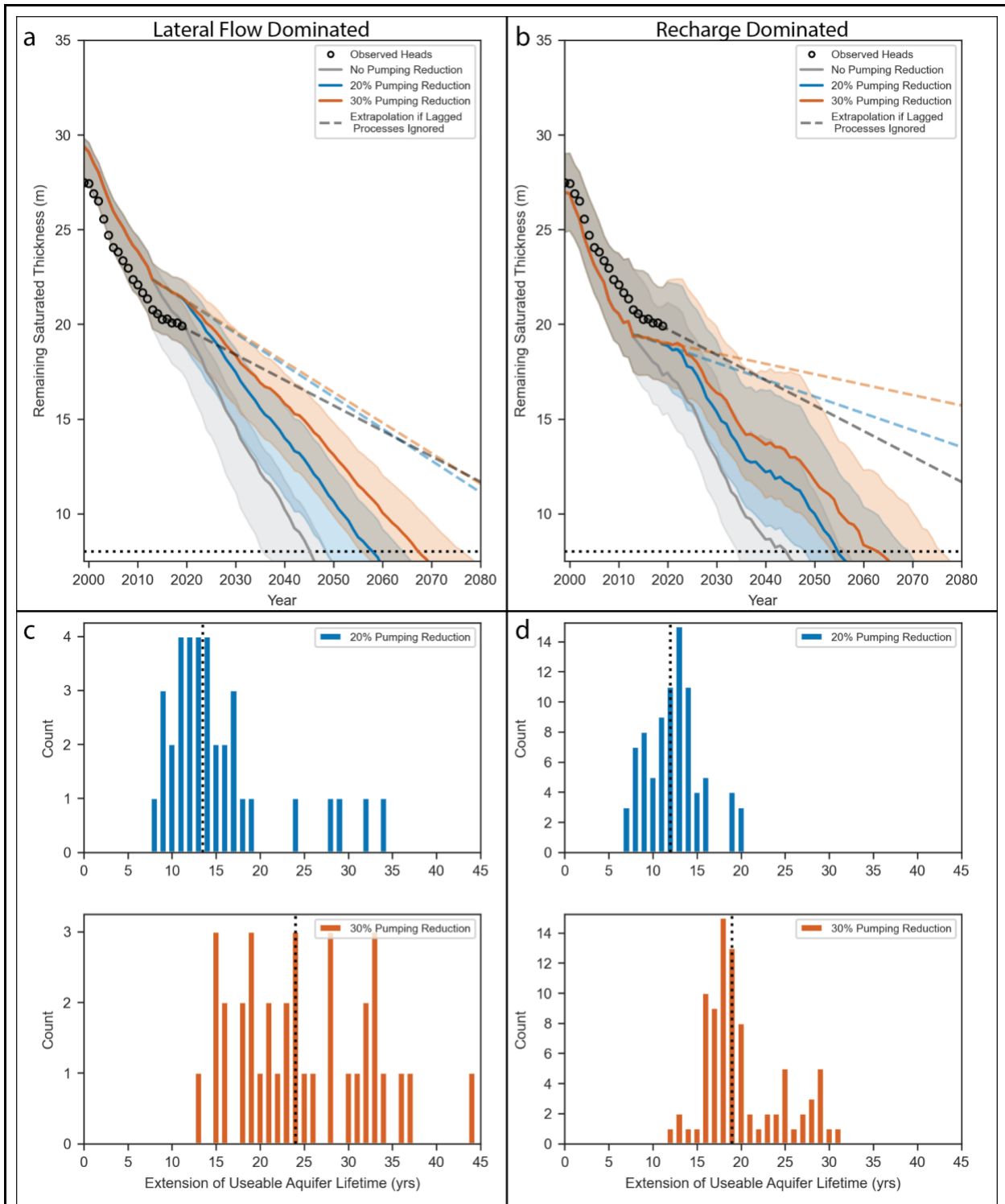


Figure 8: a) and b): Median simulated saturated thickness for the three pumping scenarios for a) lateral-flow-dominated and b) recharge-dominated cases. Dashed lines represent extrapolated remaining saturated thickness if the impact of lagged responses is ignored. The horizontal dotted line represents the minimum saturated thickness (eight meters) needed for large-scale

irrigated agriculture. c) and d): Median extension of usable lifetime (vertical black dotted line) and histogram of number of occurrences for the 20% and 30% pumping reduction scenarios for c) lateral-flow-dominated and d) recharge-dominated cases. Shaded areas in panels a) and b) represent the interquartile range of the simulated projections.

442

443

444

445

446

447

448

449

450

451

452

453

454

455

456

457

458

459

460

461

In general, these results indicate that the effectiveness of groundwater conservation could be overestimated if only using data from the period between initiation of pumping reductions and the onset of the lagged responses. Using the observed heads from 2013 to 2019 and extrapolating until the aquifer thickness drops below eight meters, the usable lifetime extends to 2107 (Figure 8a,b black dashed line). For the lateral flow-dominated cases, this value drops to 2098 for the 20% pumping reduction scenario and 2102 for the 30% pumping reduction scenario (Figure 8a, blue and orange dashed lines). The recharge-dominated cases result in a much greater duration with the usable lifetime extending to 2142 for the 20% pumping reduction case and 2220 for the 30% pumping reduction case (Figure 8b, blue and orange dashed lines). Ignoring the impacts of lagged responses by extrapolating the initial aquifer response to pumping reductions results in a dramatic overestimate of the effectiveness of these conservation methods. The subsequent increase in the water table decline rate dictates the long term effectiveness of groundwater conservation strategies. Understanding the mechanisms that control these lagged responses can manage stakeholder expectations and lead to the design of more effective conservation strategies that can further extend the usable lifetime of stressed aquifers. For example, as the effectiveness of initial conservation measures wanes and a return to increased water table decline rates begin to be observed, Butler et al. (2020b) have shown that additional pumping reductions can further extend usable aquifer lifetimes.

462 ***3.4 Implications of isolated conservation areas within heavily stressed regional aquifers***

463 Conservation strategies are most urgently needed in heavily stressed aquifers. Since
464 changes to groundwater flow can transmit the impacts of land use decisions to neighboring parts
465 of the landscape (Zipper et al., 2017), it is important to understand how impacts of pumping
466 reductions could extend beyond the borders of the conservation area. We found that changes in
467 transect-parallel lateral flow caused by conservation (Figure 7) can subsidize those outside the
468 conservation area by slowing the rate of aquifer decline in the non-conservation area (Figure 9).
469 As our modeling setup is symmetric, the largest extension of usable lifetime occurs in the center
470 of the conservation area (values plotted in Figure 8) and decreases towards and across the
471 boundary between the conservation and non-conservation areas. These cross-boundary effects
472 are greatest under the (transect-perpendicular) lateral flow-dominated cases but also occur in
473 recharge-dominated cases due to the transect-parallel lateral hydraulic gradient changes
474 discussed above. Without any reductions in pumping outside the conservation area, the non-
475 conservation area gains at least 5 years of additional usable aquifer lifetime at distances of
476 approximately 2 km from the boundary for the 20% pumping reduction case and between 3.5 and
477 4 km for the 30% pumping reduction case. Extensions of the usable aquifer lifetime at 7 km from
478 the boundary range between about 0.75 and 2 years. Effectively, the gains in usable aquifer
479 lifetime brought about by conservation can spill out of the conservation area, indicating that the
480 benefits of pumping reductions may extend beyond the borders of conservation areas by
481 subsidizing their neighbors. However, the magnitude of this effect is likely dependent on the
482 horizontal conductivity value and the size and shape of the conservation area. We would
483 anticipate a smaller transect-parallel lateral flow subsidy in areas with a lower horizontal
484 hydraulic conductivity and/or a smaller perimeter-to-area ratio relative to the conditions

485 simulated here, which would result in a longer extension of usable aquifer lifetime in the
486 conservation area.

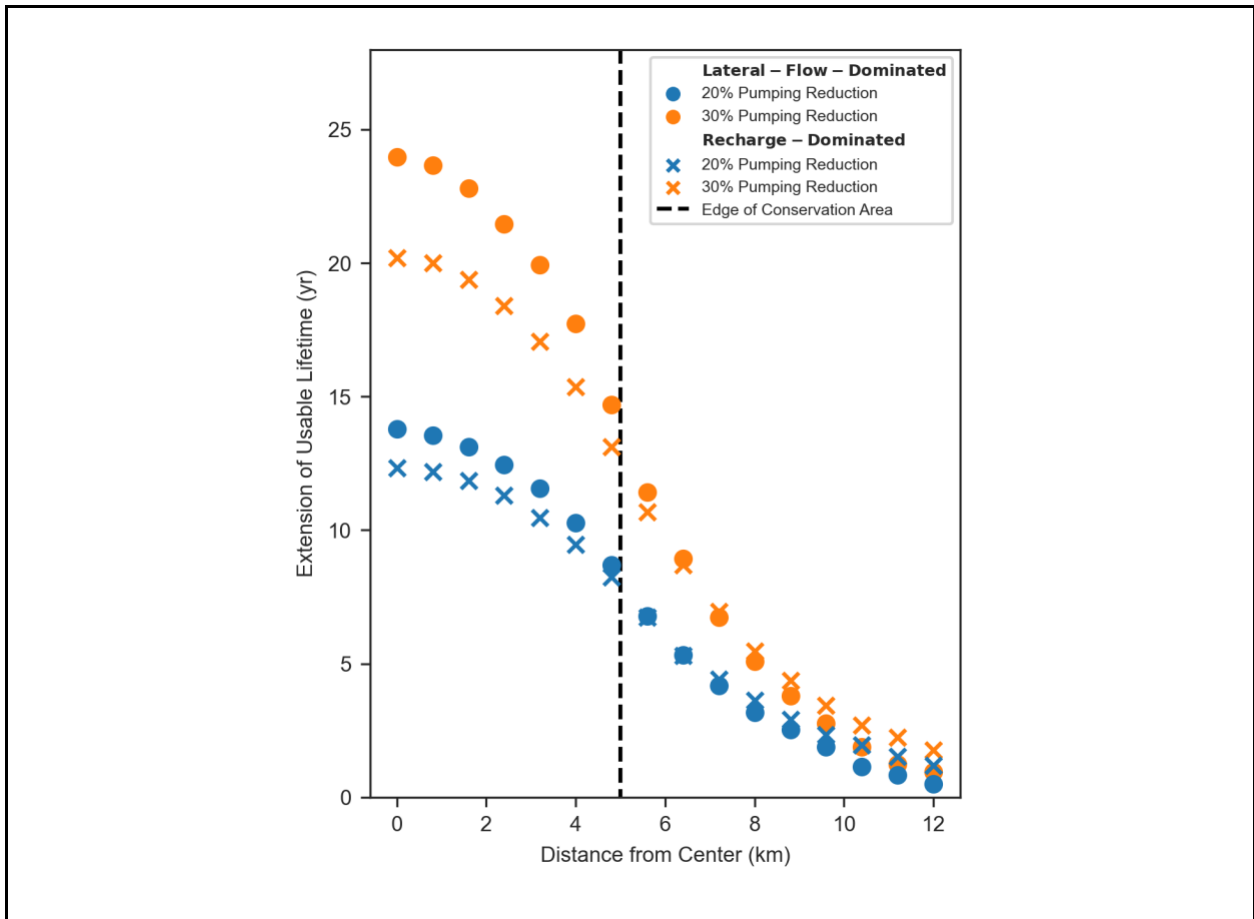


Figure 9: Average extension of usable aquifer lifetime for the lateral-flow-dominated (circles) and recharge-dominated (Xs) scenarios compared to distance from the center of the conservation area. Extension of usable aquifer lifetime was quantified for the center of each grid cell by calculating the difference in time between when the “No Conservation” scenario and the 20% and 30% pumping reduction scenarios reached eight meters of saturated thickness, which is the minimum saturated thickness capable of supporting large-scale pumping.

487
488 While our surrogate model simulations found net outflow across the LEMA boundary, in
489 practice many overexploited areas where groundwater conservation measures may be
490 implemented are closed basins and therefore this may manifest through other impacts such as a
491 reduction in cross-boundary inflows to the conservation area (Pauloo et al., 2021). In either case,

492 this indicates that the benefits of pumping reductions can extend beyond the boundaries of the
493 areas with groundwater conservation initiatives, with potential socio-political impacts. Since
494 heavily-pumped areas may preferentially exist in high productive aquifers with high
495 transmissivity, the lateral cross-boundary effects we identify here are likely possible in many
496 stressed aquifers. For instance, if pumping reductions are implemented in trans-boundary
497 aquifers, lagged responses should be accounted for to ensure that water resources are shared
498 equitably (Callegary et al., 2018; Lee et al., 2018; Lipponen & Chilton, 2018; Sindico et al.,
499 2018).

500 *3.5 Limitations and future research needs*

501 Although the modeling framework presented here reproduced the interannual and annual
502 dynamics of the observed natural system (Figure 6), there are several limitations to our approach
503 that may affect the results. First, aquifers are inherently complex, spatially heterogeneous, and
504 frequently lack sufficient observation data. Our analysis deliberately simplified this complexity
505 into a homogeneous surrogate model in order to isolate the role of lagged hydrological responses
506 to groundwater conservation, and therefore does not capture the intricacies of the natural world,
507 such as spatial changes in depth to bedrock, strata discontinuity, incorporation of regional
508 groundwater gradients, or homogeneous distributions of pumping wells. However, our sensitivity
509 analysis demonstrated that our conclusions were robust to these simplifications (see
510 Supplemental Information for details). Because our surrogate model was based on conditions of
511 a specific groundwater conservation program, the exact thresholds identified in this study may
512 not translate to other aquifer systems and should be viewed in the context of this study, which is
513 to identify how lagged processes influence groundwater conservation initiatives. However,
514 regardless of the specific thresholds, we would expect the general relationships among variables

515 to be consistent (e.g., lagged changes in recharge become more important in settings with greater
516 vertical hydraulic conductivity).

517 Second, the applied pumping and deep percolation rates are based on statistical
518 relationships using limited data. While Kansas has the most robust pumping well metering data
519 in the United States (Foster et al., 2020; USDA National Agricultural Statistics Service, 2019),
520 pumping rates for the period from 1955 to 1992 are based on a regression model while rates from
521 1993 to 2019 are based on observed data. Additionally, when developing the projected pumping
522 rates, we assumed that irrigation efficiency does not change, which may not be the case as new
523 technologies are adopted by the agricultural community. Applied deep percolation rates were
524 developed using ten years of modeled data and extrapolated to fill the historical record, which
525 may have resulted in deep percolation rates that are too high. We also assumed that the (transect-
526 perpendicular) east-to-west lateral inflows to the system are constant through time. These issues
527 point to a critical need to better monitor vertical fluxes of water in deep vadose zones and lateral
528 fluxes in aquifers to inform future modeling efforts and conservation program evaluations.

529 Third, the use of the UZF package to simulate variably saturated flow is limited in several
530 aspects. If applied deep percolation rates are greater than the prescribed saturated hydraulic
531 conductivity, excess water is removed from the system, as low hydraulic conductivity conditions
532 typical of lateral-flow-dominated cases are limited not just by the rate at which water percolates
533 through the unsaturated zone, but also by the supply of water able to infiltrate into the root zone.
534 Applying heterogeneity to the model domain was not possible with the UZF package as it can
535 only be applied to one active layer, further simplifying the representation. We had attempted to
536 address this limitation by using another MODFLOW-based variably-saturated flow solution,
537 HYDRUS Package for MODFLOW (Beegum et al., 2018; Seo et al., 2007), which solves a 1-D

538 unsaturated Richards Equation for each cell column, but experienced both instability and
539 anomalous results that prevented its application here. Finally, all projection results are based on
540 randomly sampling the historical record of precipitation to generate time series for deep
541 percolation and pumping, which provides realistic daily meteorological dynamics but inherently
542 ignores climate change impacts and implications.

543 Although our modeling approach may disregard some locally important heterogeneity,
544 our objective was to analyze the major factors controlling the long-term effectiveness of
545 groundwater conservation initiatives. Our simplified surrogate modeling approach allows for the
546 fundamental processes to be investigated while removing the impact of site specific phenomena,
547 ultimately allowing for a more generalized understanding of aquifer system dynamics that can be
548 transferred to other aquifers that are at risk of depletion. Applying these assumptions, we were
549 able to investigate the interplay among vertical hydraulic conductivity, soil water retention
550 properties, lateral flows, and recharge, the long-term effectiveness of pumping reduction based
551 groundwater conservation strategies, and estimate the extension of the usable aquifer lifetime for
552 both the lateral-flow- and recharge-dominated cases.

553 **4. Conclusions**

554 Pumping reductions are, in many settings, the only viable method for extending the
555 lifetime of groundwater resources. In this study, we demonstrate that pumping reductions can
556 lead to changes in lateral groundwater flow and recharge, and these lagged responses to pumping
557 reductions ultimately have a substantial influence over the long-term effectiveness of
558 groundwater conservation initiatives. The degree to which lateral flow and recharge impact long-
559 term effectiveness is strongly dependent on the vertical hydraulic conductivity of the unsaturated
560 zone, which controls the degree to which changes in deep percolation can translate into changes

561 in groundwater recharge. We found that larger reductions in pumping result in a longer extension
562 of the usable aquifer lifetime, and that this impact is most strongly felt in the center of the
563 conservation area and that the benefits of groundwater conservation programs may extend
564 beyond the areas implementing conservation practices. These results indicate that pumping
565 reductions can substantially extend the lifetime of heavily-stressed aquifers, but that water table
566 data from shortly after pumping reductions are enacted can overestimate the long-term
567 effectiveness of groundwater conservation.

568 **Acknowledgments**

569 This work was supported, in part, by the United States Department of Agriculture
570 (USDA) under USDA-NIFA grant 2018-67003-27406 and subaward RC104693B, the USDA
571 and the National Science Foundation (NSF) under USDA-NIFA/NSF-INFEWS grant 2018-
572 67003-27406subaward RC108063UK, and the NSF under Grant No. 2108196. Any opinions,
573 findings, and conclusions or recommendations expressed in this material are those of the authors
574 and do not necessarily reflect the views of the USDA or NSF. We would like to thank Geoff
575 Bohling and Brownie Wilson for their help procuring data and helpful comments. Data and code
576 are available at https://github.com/tomglose/SD6_Modeling_Project.git during the review
577 process and will be placed in a repository at the time of paper acceptance.

578

579 **References**

- 580 Asher, M. J., Croke, B. F. W., Jakeman, A. J., & Peeters, L. J. M. (2015). A review of surrogate
581 models and their application to groundwater modeling. *Water Resources Research*, *51*(8),
582 5957–5973. <https://doi.org/10.1002/2015WR016967>
- 583 Bailey, R. T., Morway, E. D., Niswonger, R. G., & Gates, T. K. (2013). Modeling Variably
584 Saturated Multispecies Reactive Groundwater Solute Transport with MODFLOW-UZF
585 and RT3D. *Groundwater*, *51*(5), 752–761. [https://doi.org/10.1111/j.1745-](https://doi.org/10.1111/j.1745-6584.2012.01009.x)
586 [6584.2012.01009.x](https://doi.org/10.1111/j.1745-6584.2012.01009.x)
- 587 Bakker, M., Post, V., Langevin, C. D., Hughes, J. D., White, J. T., Starn, J. J., & Fienen, M. N.
588 (2016). Scripting MODFLOW Model Development Using Python and FloPy.
589 *Groundwater*, *54*(5), 733–739. <https://doi.org/10.1111/gwat.12413>
- 590 Beegum, S., Šimůnek, J., Szymkiewicz, A., Sudheer, K. P., & Nambi, I. M. (2018). Updating the
591 Coupling Algorithm between HYDRUS and MODFLOW in the HYDRUS Package for
592 MODFLOW. *Vadose Zone Journal*, *17*(1), 180034.
593 <https://doi.org/10.2136/vzj2018.02.0034>
- 594 Beven, K. (2006). A manifesto for the equifinality thesis. *The Model Parameter Estimation*
595 *Experiment*, *320*(1), 18–36. <https://doi.org/10.1016/j.jhydrol.2005.07.007>
- 596 Bierkens, M. F. P., & Wada, Y. (2019). Non-renewable groundwater use and groundwater
597 depletion: a review. *Environmental Research Letters*, *14*(6), 063002.
598 <https://doi.org/10.1088/1748-9326/ab1a5f>
- 599 Brooks, R. H., & Corey, A. T. (1966). Properties of porous media affecting fluid flow. *Journal of*
600 *the Irrigation and Drainage Division*, *92*(2), 61–90.
- 601 Butler, J. J., Jr., Whittemore, D. O., Wilson, B. B., & Bohling, G. C. (2016). A new approach for

602 assessing the future of aquifers supporting irrigated agriculture. *Geophysical Research*
603 *Letters*, 43(5), 2004–2010. <https://doi.org/10.1002/2016GL067879>

604 Butler, J. J., Jr., Whittemore, D. O., Reboulet, E. C., Knobbe, S., Wilson, B. B., & Bohling, G. C.
605 (2019). High Plains aquifer index well program: 2019 annual report.

606 Butler, J. J., Jr., Bohling, G. C., Whittemore, D. O., & Wilson, B. B. (2020a). A roadblock on the
607 path to aquifer sustainability: underestimating the impact of pumping reductions.
608 *Environmental Research Letters*, 15(1), 014003. [https://doi.org/10.1088/1748-](https://doi.org/10.1088/1748-9326/ab6002)
609 [9326/ab6002](https://doi.org/10.1088/1748-9326/ab6002)

610 Butler, J. J., Jr., Bohling, G. C., Whittemore, D. O., & Wilson, B. B. (2020b). Charting Pathways
611 Toward Sustainability for Aquifers Supporting Irrigated Agriculture. *Water Resources*
612 *Research*, 56(10), e2020WR027961. <https://doi.org/10.1029/2020WR027961>

613 Callegary, J. B., Megdal, S. B., Tapia Villaseñor, E. M., Petersen-Perlman, J. D., Minjárez Sosa,
614 I., Monreal, R., et al. (2018). Findings and lessons learned from the assessment of the
615 Mexico-United States transboundary San Pedro and Santa Cruz aquifers: The utility of
616 social science in applied hydrologic research. *Special Issue on International Shared*
617 *Aquifer Resources Assessment and Management*, 20, 60–73.
618 <https://doi.org/10.1016/j.ejrh.2018.08.002>

619 Castilla-Rho, J. C., Rojas, R., Andersen, M. S., Holley, C., & Mariethoz, G. (2019). Sustainable
620 groundwater management: How long and what will it take? *Global Environmental*
621 *Change*, 58, 101972. <https://doi.org/10.1016/j.gloenvcha.2019.101972>

622 Deines, J. M., Kendall, A. D., Butler, J. J., Jr., & Hyndman, D. W. (2019). Quantifying irrigation
623 adaptation strategies in response to stakeholder-driven groundwater management in the
624 US High Plains Aquifer. *Environmental Research Letters*, 14, 044014.

625 <https://doi.org/10.1088/1748-9326/aafe39>

626 Deines, J. M., Schipanski, M. E., Golden, B., Zipper, S. C., Nozari, S., Rottler, C., et al. (2020).
627 Transitions from irrigated to dryland agriculture in the Ogallala Aquifer: Land use
628 suitability and regional economic impacts. *Agricultural Water Management*, 233,
629 106061. <https://doi.org/10.1016/j.agwat.2020.106061>

630 Deines, J. M., Kendall, A. D., Butler, J. J., Jr., Basso, B., & Hyndman, D. W. (2021). Combining
631 Remote Sensing and Crop Models to Assess the Sustainability of Stakeholder-Driven
632 Groundwater Management in the US High Plains Aquifer. *Water Resources Research*,
633 e2020WR027756. <https://doi.org/10.1029/2020WR027756>

634 DeSimone, L. A., McMahon, P. B., & Rosen, M. R. (2015). *The quality of our Nation's waters:*
635 *Water quality in principal aquifers of the United States, 1991-2010* (Report No. 1360) (p.
636 161). Reston, VA. <https://doi.org/10.3133/cir1360>

637 Dieter, C. A., Maupin, M. A., Caldwell, R. R., Harris, M. A., Ivahnenko, T. I., Lovelace, J. K., et
638 al. (2018). *Estimated use of water in the United States in 2015* (Report No. 1441) (p. 76).
639 Reston, VA. <https://doi.org/10.3133/cir1441>

640 Doherty, J. (2015). *Calibration and uncertainty analysis for complex environmental models*.
641 Watermark Numerical Computing Brisbane, Australia.

642 Foster, T., Brozović, N., & Butler, A. P. (2017). Effects of initial aquifer conditions on economic
643 benefits from groundwater conservation. *Water Resources Research*, 53(1), 744–762.
644 <https://doi.org/10.1002/2016WR019365>

645 Foster, T., Mieno, T., & Brozović, N. (2020). Satellite-Based Monitoring of Irrigation Water
646 Use: Assessing Measurement Errors and Their Implications for Agricultural Water
647 Management Policy. *Water Resources Research*, 56(11), e2020WR028378.

648 <https://doi.org/10.1029/2020WR028378>

649 Fross, D., Sophocleous, M. A., Wilson, B. B., & Butler, J. J., Jr. (2012). Kansas High Plains
650 Aquifer Atlas, Kansas Geological Survey. Retrieved from
651 http://www.kgs.ku.edu/HighPlains/HPA_Atlas/index.html

652 Gleeson, T., Alley, W. M., Allen, D. M., Sophocleous, M. A., Zhou, Y., Taniguchi, M., &
653 VanderSteen, J. (2012). Towards sustainable groundwater use: setting long-term goals,
654 backcasting, and managing adaptively. *Ground Water*, 50(1), 19–26.
655 <https://doi.org/10.1111/j.1745-6584.2011.00825.x>

656 Gleeson, T., Cuthbert, M., Ferguson, G., & Perrone, D. (2020). Global Groundwater
657 Sustainability, Resources, and Systems in the Anthropocene. *Annual Review of Earth and*
658 *Planetary Sciences*, 48(1), 431–463. [https://doi.org/10.1146/annurev-earth-071719-](https://doi.org/10.1146/annurev-earth-071719-055251)
659 [055251](https://doi.org/10.1146/annurev-earth-071719-055251)

660 Golden, B. (2018). *Monitoring the Impacts of Sheridan County 6 Local Enhanced Management*
661 *Area: Final Report for 2013 – 2017*. Manhattan, KS. Retrieved from
662 [https://agriculture.ks.gov/docs/default-source/dwr-water-appropriation-](https://agriculture.ks.gov/docs/default-source/dwr-water-appropriation-documents/sheridancounty6_lemma_goldenreport_2013-2017.pdf?sfvrsn=dac48ac1_0)
663 [documents/sheridancounty6_lemma_goldenreport_2013-2017.pdf?sfvrsn=dac48ac1_0](https://agriculture.ks.gov/docs/default-source/dwr-water-appropriation-documents/sheridancounty6_lemma_goldenreport_2013-2017.pdf?sfvrsn=dac48ac1_0)

664 Gurdak, J. J., Walvoord, M. A., & McMahon, P. B. (2008). Susceptibility to Enhanced Chemical
665 Migration from Depression-Focused Preferential Flow, High Plains Aquifer. *Vadose*
666 *Zone Journal*, 7(4), 1218–1230. <https://doi.org/10.2136/vzj2007.0145>

667 Hansen, C. V. (1991). *Estimates of freshwater storage and potential natural recharge for*
668 *principal aquifers in Kansas* (Report No. 87–4230). <https://doi.org/10.3133/wri874230>

669 Hou, X., Wang, S., Jin, X., Li, M., Lv, M., & Feng, W. (2020). Using an ETWatch (RS)-UZP-
670 MODFLOW Coupled Model to Optimize Joint Use of Transferred Water and Local

671 Water Sources in a Saline Water Area of the North China Plain. *Water*, 12(12), 3361.

672 Hu, Y., Moiwo, J. P., Yang, Y., Han, S., & Yang, Y. (2010). Agricultural water-saving and
673 sustainable groundwater management in Shijiazhuang Irrigation District, North China
674 Plain. *Journal of Hydrology*, 393(3), 219–232.
675 <https://doi.org/10.1016/j.jhydrol.2010.08.017>

676 Huggins, X., Gleeson, T., Kumm, M., Zipper, S. C., Wada, Y., Troy, T. J., & Famiglietti, J. S.
677 (2022). Hotspots for social and ecological impacts from freshwater stress and storage
678 loss. *Nature Communications*, 13(1), 439. <https://doi.org/10.1038/s41467-022-28029-w>

679 Hunt, R. J., Prudic, D. E., Walker, J. F., & Anderson, M. P. (2008). Importance of Unsaturated
680 Zone Flow for Simulating Recharge in a Humid Climate. *Groundwater*, 46(4), 551–560.
681 <https://doi.org/10.1111/j.1745-6584.2007.00427.x>

682 Kansas Department of Agriculture. (2013). Order of designation approving the Sheridan 6 Local
683 Enhanced Management Area within Groundwater Management District No. 4. Retrieved
684 from [https://sftp.kda.ks.gov:4443/LEMAs/SD6/LEMA.SD6.OrderOfDesignation.2013](https://sftp.kda.ks.gov:4443/LEMAs/SD6/LEMA.SD6.OrderOfDesignation.20130417.pdf)
685 [0417.pdf](https://sftp.kda.ks.gov:4443/LEMAs/SD6/LEMA.SD6.OrderOfDesignation.20130417.pdf)

686 Kansas Department of Agriculture. (2018). Order of designation regarding the Groundwater
687 Management District No. 4 District Wide Local Enhanced Management Plan. Retrieved
688 from [https://agriculture.ks.gov/docs/default-source/dwr-water-appropriation-](https://agriculture.ks.gov/docs/default-source/dwr-water-appropriation-documents/gmd4_lemma_orderofdesignation.pdf?sfvrsn=30e981c1_4)
689 [documents/gmd4_lemma_orderofdesignation.pdf?sfvrsn=30e981c1_4](https://agriculture.ks.gov/docs/default-source/dwr-water-appropriation-documents/gmd4_lemma_orderofdesignation.pdf?sfvrsn=30e981c1_4)

690 Kansas Department of Agriculture. (2021). Order of designation regarding the Management Plan
691 for the Wichita County Local Enhanced Management Area. Retrieved from
692 [https://agriculture.ks.gov/docs/default-source/dwr-water-appropriation-documents/whc-](https://agriculture.ks.gov/docs/default-source/dwr-water-appropriation-documents/whc-lemma-order-of-designation---final.pdf?sfvrsn=60d690c1_0)
693 [lemma-order-of-designation---final.pdf?sfvrsn=60d690c1_0](https://agriculture.ks.gov/docs/default-source/dwr-water-appropriation-documents/whc-lemma-order-of-designation---final.pdf?sfvrsn=60d690c1_0)

694 Kansas Statutes Annotated 82a-1041. (2012). Local enhanced management areas; establishment
695 procedures; duties of chief engineer; hearing; notice; orders; review. Retrieved from
696 http://www.ksrevisor.org/statutes/chapters/ch82a/082a_010_0041.html

697 Katz, B. S., Stotler, R. L., Hirmas, D., Ludvigson, G., Smith, J. J., & Whittemore, D. O. (2016).
698 Geochemical Recharge Estimation and the Effects of a Declining Water Table. *Vadose*
699 *Zone Journal*, 15(vzj2016.04.0031). <https://doi.org/10.2136/vzj2016.04.0031>

700 Kennedy, J., Ferré, T. P. A., & Creutzfeldt, B. (2016). Time-lapse gravity data for monitoring
701 and modeling artificial recharge through a thick unsaturated zone. *Water Resources*
702 *Research*, 52(9), 7244–7261. <https://doi.org/10.1002/2016WR018770>

703 Kling, H., Fuchs, M., & Paulin, M. (2012). Runoff conditions in the upper Danube basin under
704 an ensemble of climate change scenarios. *Journal of Hydrology*, 424–425, 264–277.
705 <https://doi.org/10.1016/j.jhydrol.2012.01.011>

706 Konikow, L. F., & Bredehoeft, J. D. (1992). Ground-water models cannot be validated.
707 *Validation of Geo-Hydrological Models Part 1*, 15(1), 75–83.
708 [https://doi.org/10.1016/0309-1708\(92\)90033-X](https://doi.org/10.1016/0309-1708(92)90033-X)

709 Lee, E., Jayakumar, R., Shrestha, S., & Han, Z. (2018). Assessment of transboundary aquifer
710 resources in Asia: Status and progress towards sustainable groundwater management.
711 *Special Issue on International Shared Aquifer Resources Assessment and Management*,
712 20, 103–115. <https://doi.org/10.1016/j.ejrh.2018.01.004>

713 Lin, X., Harrington, J., Ciampitti, I., Gowda, P., Brown, D., & Kisekka, I. (2017). Kansas Trends
714 and Changes in Temperature, Precipitation, Drought, and Frost-Free Days from the 1890s
715 to 2015. *Journal of Contemporary Water Research & Education*, 162(1), 18–30.
716 <https://doi.org/10.1111/j.1936-704X.2017.03257.x>

717 Lipponen, A., & Chilton, J. (2018). Development of cooperation on managing transboundary
718 groundwaters in the pan-European region: The role of international frameworks and joint
719 assessments. *Special Issue on International Shared Aquifer Resources Assessment and*
720 *Management*, 20, 145–157. <https://doi.org/10.1016/j.ejrh.2018.05.001>

721 Liu, G., Wilson, B. B., Bohling, G. C., Whittemore, D. O., & Butler Jr, J. J. (2022). Estimation
722 of Specific Yield for Regional Groundwater Models: Pitfalls, Ramifications, and a
723 Promising Path Forward. *Water Resources Research*, 58(1), e2021WR030761.
724 <https://doi.org/10.1029/2021WR030761>

725 McKay, M. D., Beckman, R. J., & Conover, W. J. (1979). Comparison of Three Methods for
726 Selecting Values of Input Variables in the Analysis of Output from a Computer Code.
727 *Technometrics*, 21(2), 239–245. <https://doi.org/10.1080/00401706.1979.10489755>

728 McMahon, P. B., Dennehy, K. F., Bruce, B. W., Böhlke, J. K., Michel, R. L., Gurdak, J. J., &
729 Hurlbut, D. B. (2006). Storage and transit time of chemicals in thick unsaturated zones
730 under rangeland and irrigated cropland, High Plains, United States. *Water Resources*
731 *Research*, 42(3). <https://doi.org/10.1029/2005WR004417>

732 Miro, M. E., & Famiglietti, J. S. (2019). A framework for quantifying sustainable yield under
733 California’s Sustainable Groundwater Management Act (SGMA). *Sustainable Water*
734 *Resources Management*, 5(3), 1165–1177.

735 Morway, E. D., Niswonger, R. G., Langevin, C. D., Bailey, R. T., & Healy, R. W. (2013).
736 Modeling Variably Saturated Subsurface Solute Transport with MODFLOW-UZF and
737 MT3DMS. *Groundwater*, 51(2), 237–251. [https://doi.org/10.1111/j.1745-](https://doi.org/10.1111/j.1745-6584.2012.00971.x)
738 [6584.2012.00971.x](https://doi.org/10.1111/j.1745-6584.2012.00971.x)

739 Nazarieh, F., Ansari, H., Ziaei, A. N., Izady, A., Davari, K., & Brunner, P. (2018). Spatial and

740 temporal dynamics of deep percolation, lag time and recharge in an irrigated semi-arid
741 region. *Hydrogeology Journal*, 26(7), 2507–2520. <https://doi.org/10.1007/s10040-018->
742 1789-z

743 Niswonger, R. G., & Prudic, D. E. (2009). Comment on “Evaluating Interactions between
744 Groundwater and Vadose Zone Using the HYDRUS-Based Flow Package for
745 MODFLOW” by Navin Kumar C. Twarakavi, Jirka Šimůnek, and Sophia Seo. *Vadose*
746 *Zone Journal*, 8(3), 818–819. <https://doi.org/10.2136/vzj2008.0155>

747 Niswonger, R. G., Prudic, D. E., & Regan, R. S. (2006). *Documentation of the Unsaturated-Zone*
748 *Flow (UZFI) Package for modeling Unsaturated Flow Between the Land Surface and the*
749 *Water Table with MODFLOW-2005* (Report No. 6-A19). <https://doi.org/10.3133/tm6A19>

750 Pauloo, R. A., Fogg, G. E., Guo, Z., & Harter, T. (2021). Anthropogenic basin closure and
751 groundwater salinization (ABCSAL). *Journal of Hydrology*, 593, 125787.
752 <https://doi.org/10.1016/j.jhydrol.2020.125787>

753 Pfeiffer, L., & Lin, C.-Y. C. (2010). The effect of irrigation technology on groundwater use.
754 *Choices*, 25(3), 1–6.

755 Poeter, E. P., & Hill, M. C. (1999). UCODE, a computer code for universal inverse modeling.
756 *Computers & Geosciences*, 25(4), 457–462.

757 Razavi, S., Tolson, B. A., & Burn, D. H. (2012). Review of surrogate modeling in water
758 resources. *Water Resources Research*, 48(7). <https://doi.org/10.1029/2011WR011527>

759 Rogers, D. H., & Lamm, F. R. (2012). Kansas irrigation trends. Presented at the Proceedings of
760 the 24th Annual Central Plains Irrigation Conference, Colby, Kansas, February 21-22,
761 2012, Central Plains Irrigation Association.

762 Savenije, H. H. G. (2001). Equifinality, a blessing in disguise? *Hydrological Processes*, 15(14),

763 2835–2838. <https://doi.org/10.1002/hyp.494>

764 Scanlon, B. R., Keese, K. E., Flint, A. L., Flint, L. E., Gaye, C. B., Edmunds, W. M., &
765 Simmers, I. (2006). Global synthesis of groundwater recharge in semiarid and arid
766 regions. *Hydrological Processes*, 20(15), 3335–3370. <https://doi.org/10.1002/hyp.6335>

767 Scanlon, B. R., Faunt, C. C., Longuevergne, L., Reedy, R. C., Alley, W. M., McGuire, V. L., &
768 McMahon, P. B. (2012). Groundwater depletion and sustainability of irrigation in the US
769 High Plains and Central Valley. *Proceedings of the National Academy of Sciences*,
770 109(24), 9320–9325. <https://doi.org/10.1073/pnas.1200311109>

771 Seo, H. S., Simunek, J., & Poeter, E. P. (2007). Documentation of the hydrus package for
772 modflow-2000, the us geological survey modular ground-water model. *IGWMC-*
773 *International Ground Water Modeling Center*.

774 Sindico, F., Hirata, R., & Manganelli, A. (2018). The Guarani Aquifer System: From a Beacon
775 of hope to a question mark in the governance of transboundary aquifers. *Special Issue on*
776 *International Shared Aquifer Resources Assessment and Management*, 20, 49–59.
777 <https://doi.org/10.1016/j.ejrh.2018.04.008>

778 Smith, R. (1983). Approximate soil water movement by kinematic characteristics. *Soil Science*
779 *Society of America Journal*, 47(1), 3–8.

780 Smith, R., & Hebbert, R. H. B. (1983). Mathematical simulation of interdependent surface and
781 subsurface hydrologic processes. *Water Resources Research*, 19(4), 987–1001.
782 <https://doi.org/10.1029/WR019i004p00987>

783 USDA National Agricultural Statistics Service. (2019). 2018 Irrigation and water management
784 survey, 3. Retrieved from
785 https://www.nass.usda.gov/Publications/AgCensus/2017/Online_Resources/Farm_and_R

786 anch_Irrigation_Survey/fris.pdf

787 Voss, C. I. (2011a). Editor's message: Groundwater modeling fantasies —part 1, adrift in the
788 details. *Hydrogeology Journal*, 19(7), 1281–1284. [https://doi.org/10.1007/s10040-011-](https://doi.org/10.1007/s10040-011-0789-z)
789 0789-z

790 Voss, C. I. (2011b). Editor's message: Groundwater modeling fantasies—part 2, down to earth.
791 *Hydrogeology Journal*, 19(8), 1455–1458. <https://doi.org/10.1007/s10040-011-0790-6>

792 Whittemore, D. O., Butler, J. J., Jr., & Wilson, B. B. (2018). Status of the High Plains Aquifer in
793 Kansas. *Kansas Geological Survey Technical Series*, 22. Retrieved from
794 www.kgs.ku.edu/Publications/Bulletins/TS22/index.html

795 Zell, W. O., & Sanford, W. E. (2020). Calibrated Simulation of the Long-Term Average Surficial
796 Groundwater System and Derived Spatial Distributions of its Characteristics for the
797 Contiguous United States. *Water Resources Research*, 56(8), e2019WR026724.
798 <https://doi.org/10.1029/2019WR026724>

799 Zipper, S. C., Soylu, M. E., Kucharik, C. J., & II, S. P. L. (2017). Quantifying indirect
800 groundwater-mediated effects of urbanization on agroecosystem productivity using
801 MODFLOW-AgroIBIS (MAGI), a complete critical zone model. *Ecological Modelling*,
802 359, 201–219. <https://doi.org/10.1016/j.ecolmodel.2017.06.002>

803 Zipper, S. C., Lamontagne-Hallé, P., McKenzie, J. M., & Rocha, A. V. (2018). Groundwater
804 Controls on Postfire Permafrost Thaw: Water and Energy Balance Effects. *Journal of*
805 *Geophysical Research: Earth Surface*, 123(10), 2677–2694.
806 <https://doi.org/10.1029/2018JF004611>

807 Zipper, S. C., Gleeson, T., Kerr, B., Howard, J. K., Rohde, M. M., Carah, J., & Zimmerman, J.
808 (2019). Rapid and Accurate Estimates of Streamflow Depletion Caused by Groundwater

809 Pumping Using Analytical Depletion Functions. *Water Resources Research*, 55(7), 5807–
810 5829. <https://doi.org/10.1029/2018WR024403>